Liquid Crystals
Publication details, including instructions for authors and subscription information:
http://www.informaworld.com/smpp/title~content=t713926090

Phase transitions and molecular properties of new divinyl and diepoxy compounds

M. Wlodarska[a]; B. Mossety-Leszczak[b]; H. Galina[b]; G. W. Bak Corresponding author[a]; T. Pakula[c]
[a] Institute of Physics, Technical University of Lodz, 93-005 Lodz, Poland [b] Department of Industrial and Materials Chemistry, Rzeszow University of Technology, 35-959 Rzeszow, Poland [c] Max-Planck-Institute for Polymer Research, 65021 Mainz, Germany

Online publication date: 12 May 2010

To cite this Article Wlodarska, M. , Mossety-Leszczak, B. , Galina, H. , Bak Corresponding author, G. W. and Pakula, T.(2004) 'Phase transitions and molecular properties of new divinyl and diepoxy compounds', Liquid Crystals, 31: 4, 525 — 534
To link to this Article: DOI: 10.1080/02678290410001648615
URL: http://dx.doi.org/10.1080/02678290410001648615

LIQUID CRYSTALS, VOL. 31, NO. 4, APRIL 2004, 525–534

Phase transitions and molecular properties of new divinyl and diepoxy compounds

M. WLODARSKA, B. MOSSETY-LESZCZAK†, H. GALINA†, G. W. BAK* and T. PAKULA‡

Institute of Physics, Technical University of Lodz, 93-005 Lodz, Poland
†Department of Industrial and Materials Chemistry, Rzeszow University of Technology, 35-959 Rzeszow, Poland
‡Max-Planck-Institute for Polymer Research, Postfach 3148, 65021 Mainz, Germany

(*Received 28 October 2002; in final form 7 October 2003; accepted 20 October 2003*)

The aim of this paper is to compare some physical properties of six new divinyl and diepoxy compounds. The compounds differ in the length of the rigid central segments. Optical observations and differential scanning calorimetry confirmed the existence of a mesophase in five compounds and enabled the determination of the phase transition temperatures. The wide angle X-ray scattering (WAXS) measurements of samples aligned in a magnetic field and the optical observations allowed the identification of the mesophase types. In four compounds a nematic mesophase was detected during both heating and cooling. In one case two higher ordered phases were observed during cooling. The analysis of WAXS images and the positions and shapes of the scattering intensity peaks suggests a smectic B–crystal E transition. Using the data obtained in WAXS measurements carried out in the nematic phase, the lengths of the molecules and the average nearest neighbour distances were estimated. The average intermolecular distances and the layer spacings were also estimated for the SmB and E phases. The lengths of the molecules were also calculated by means of theoretical *ab initio* methods. The results obtained are in very good agreement with the experimental data.

1. Introduction

Liquid crystalline (LC) materials are widely used in modern technologies since their first application in electro-optical displays. Despite more than 30 years of development of LC displays, there is a continuing interest in these materials due to the increasing demand for hand-held devices requiring lightweight and low power displays. In any innovative liquid crystalline device, novel components and materials also play important roles [1].

The aim of this paper is to present the synthesis and the basic physical properties of new divinyl and diepoxy materials [2]. The data presented include the results of optical and differential scanning calorimetry (DSC) measurements, which allowed the precise determination of phase transitions. Wide angle X-ray scattering (WAXS) measurements confirmed the type of the mesophase. The approximate lengths of the molecules and the average distances between them were also obtained in these studies. The molecular lengths were compared with values computed theoretically with the use of *ab initio* methods [3–5].

*Author for correspondence; e-mail: gwbak@p.lodz.pl

2. Materials

The compounds investigated belong to newly synthesized [2] series of divinyl and diepoxy compounds which differ in the length of the rigid segment. Their molecular structures are shown in figure 1.

The acronyms **B1**, **M1** and **M2** are used to denote the three divinyl molecules with differing central segments, while the molecules with epoxy terminal groups are denoted by **BU1**, **MU1** and **MU2**.

Earlier investigations using *ab initio* methods [4, 5] resulted in establishing the geometry of the molecules **M2**, **MU2**, **M1**, **MU1**, **B1** and **BU1**. The calculations were carried out for a single molecule, taking no account of any interactions with other molecules or with the surrounding medium. The calculations indicated that the central segment of the **B1**/**BU1** molecules may exist in two stable conformations differing in the mutual orientation of the C–O groups. As a result, eight different structures (**B1**$_\alpha$, **B1**$_\beta$, **M1**, **M2**, **BU1**$_\alpha$,

Liquid Crystals ISSN 0267-8292 print/ISSN 1366-5855 online © 2004 Taylor & Francis Ltd
http://www.tandf.co.uk/journals
DOI: 10.1080/02678290410001648615

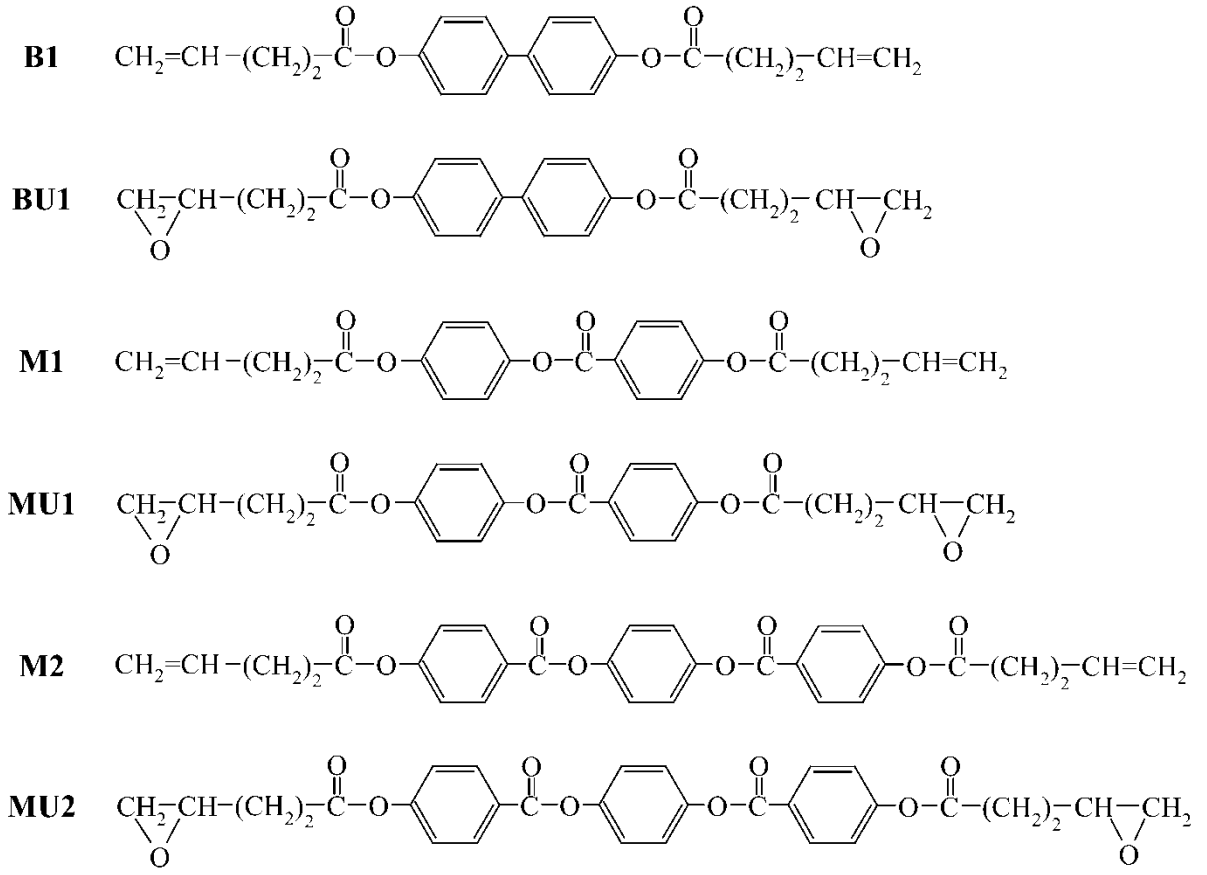

Figure 1. Molecular structures of the compounds investigated.

BU1$_\beta$, **MU1** and **MU2**) had to be considered in our further analysis (in 'α' structures both carbonyl groups are aligned in the same direction, while in 'β' structures, they are aligned in opposite directions). For all the molecules investigated the calculations showed the existence of several molecular conformers with very similar energy values which may coexist in real materials.

3. Experimental

3.1. *Characterization*

The chemical structures of the products of synthesis were confirmed by ^{1}H NMR and IR spectroscopy, using a Tesla BS 587A 80 Hz and a Paragon 1000 FTIR spectrometer, respectively. Elemental analysis was performed with elemental analyser EA 1108 (Carlo Erba). The purity of the epoxy compounds was chemically assessed by the titration of a chloroform solution containing tetraethylammonium bromide with perchloric acid solution in anhydrous acetic acid. The procedure described in the standard ISO 3001-1978 was used. The measured epoxy numbers (in moles of epoxy groups per 100 g) differed from the calculated values by less than 1% (1.3% for **MU2**).

The textures of the compounds were observed using a Zeiss polarizing microscope at a magnification of $80\times$, with crossed polarizers. The temperature was controlled by means of a Linkam TMS 91 hot stage. The measurements were carried out in cells composed of parallel glass plates covered with conducting layers. The sample thickness of the cell was approximately 6×10^{-5} m.

DSC measurements were performed with the use of a Mettler Toledo DSC30 instrument under nitrogen atmosphere. The thermograms recorded at heating and cooling rate of $2\,\mathrm{deg\,min^{-1}}$ allowed for the determination of phase transitions.

WAXS measurements were conducted using a rotating anode (Rigaku 18 kW) X-ray beam with pinhole collimation and a two-dimensional detector (Siemens) with 1024×1024 pixels. A double graphite monochromator for the Cu K_α radiation ($\lambda=0.154$ nm) was used. The beam diameter was about 0.5 mm and the sample to detector distance was 80 mm. Measurements were performed at various temperatures for samples melted in glass capillaries and aligned in a magnetic field.

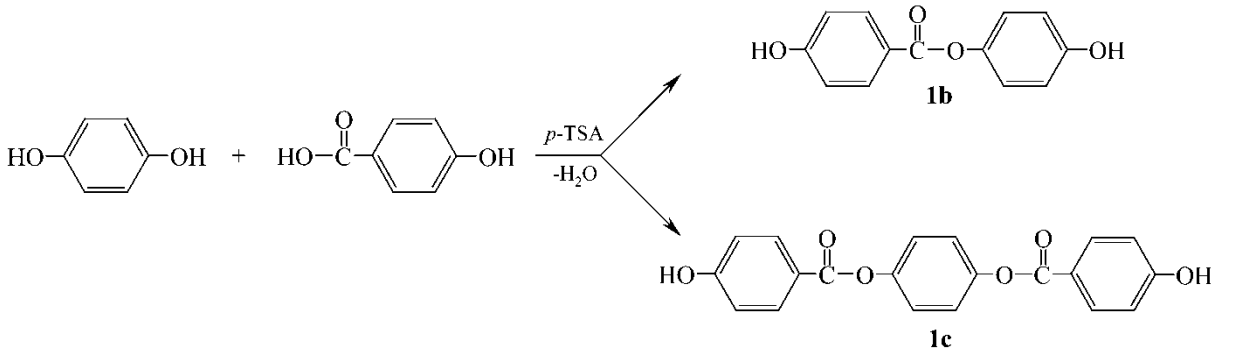

Scheme 1.

The *ab initio* calculations were conducted using a restricted Hartree–Fock (RHF) method with 6-31G(d) standard basis set. The structures of all molecules were optimized to a minimum of energy using the Berny algorithm [6]. All the computations were carried out using the *Gaussian 98* program suite [3] running on a PC workstation.

3.2. *Synthesis*

All the starting materials were commercial reagents (Aldrich, Fluka, Merck) and used without further purification. The rigid segments were 4,4′-biphenol (**1a**), 4-hydroxyphenyl-4-hydroxybenzoate (**1b**) and bis(4′-hydroxybenzoyl) 1,4-dihydroxybenzene (**1c**). **1a** was a commercial product; **1b** and **1c** were obtained by esterification of 4-hydroxybenzoic acid with hydroquinone in the presence of a catalytic amount of *p*-toluenesulphonic acid (*p*-TSA) by applying a procedure similar to that described by Kangas *et al.* [7], see scheme 1. 4-Pentenoic acid (**2**) was obtained in the so-called malonic synthesis described, for example by Bochwic [8]. The synthetic route used in our study is outlined in scheme 2.

3.3. *Esterification*

To 0.1 mol of mesogenic diol (1.86 g of **1a**, 2.30 g of **1b** or 3.5 g of **1c**) and 0.02 mol (2.00 g) of 4-pentenoic acid **2** in 100 cm^3 of dry dichloromethane, 0.022 mol

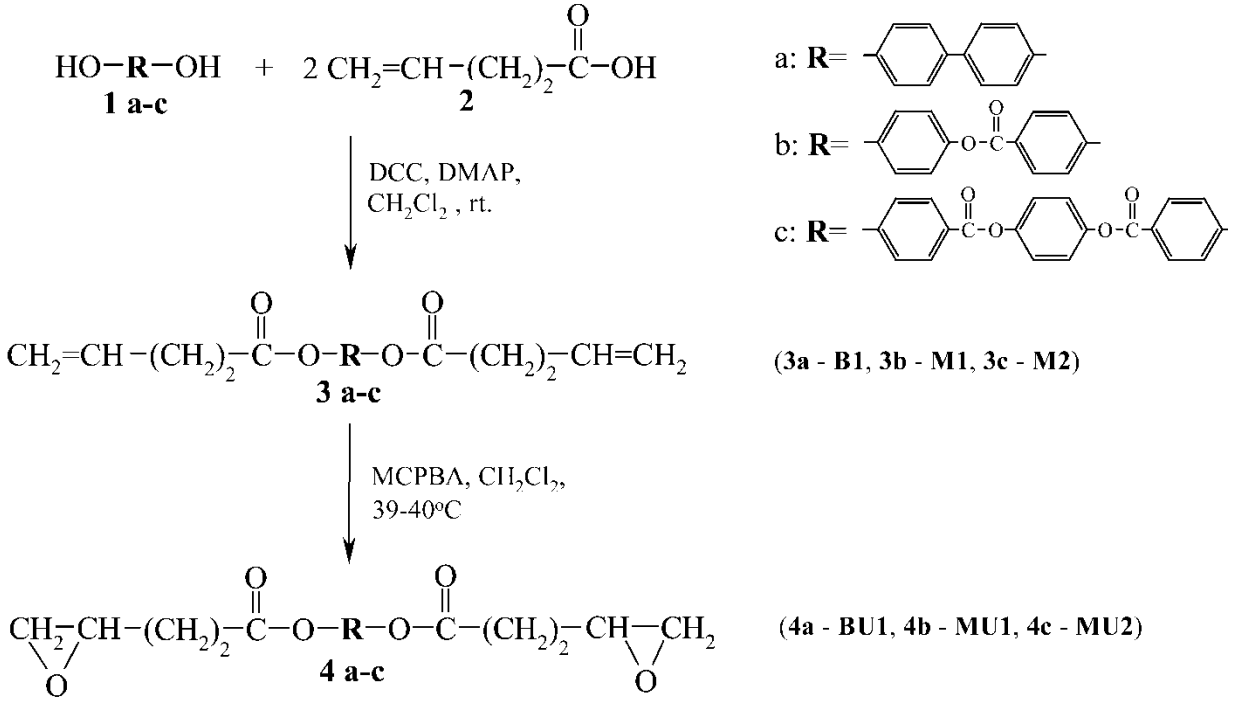

Scheme 2.

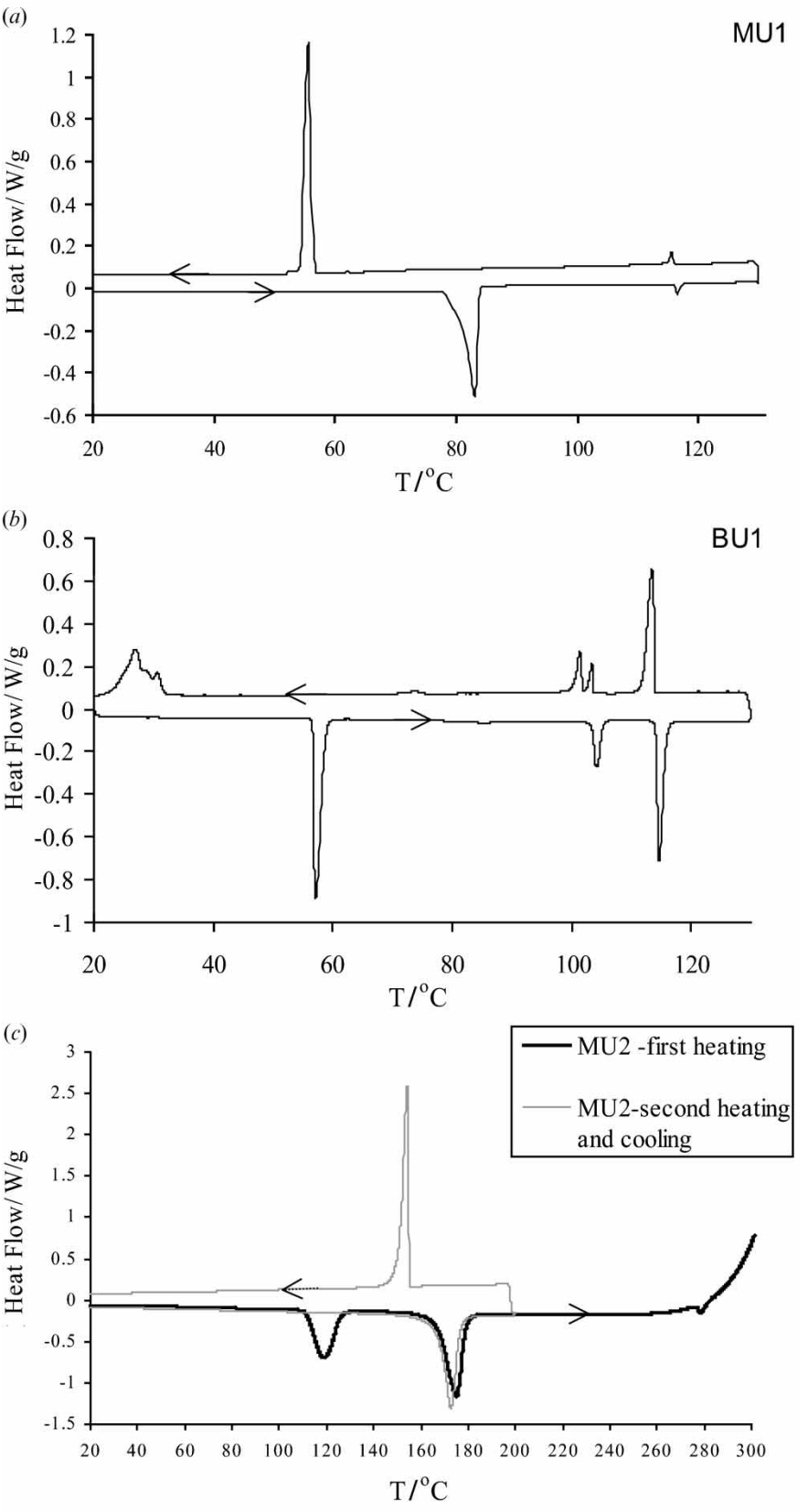

Figure 2. Representative DSC traces of: (*a*) **MU1**, heating and cooling rate of 2 deg min^{-1}; (*b*) **BU1**, heating and cooling rate of 2 deg min^{-1}; (*c*) **MU2**, first curve recorded during heating until degradation of the material began, second curve recorded during subsequent heating and cooling at 2 deg min^{-1}, after initial heating to 200°C. The arrows show the direction of heat flow (heating/cooling).

(4.54 g) of *N*,*N*-dicyclohexylcarbodiimide, and a catalytic amount (8×10^{-4} mol, 0.0977 g) of 4-dimethylaminopyridine were added. The reaction mixture was stirred for 24 h, then *N*,*N*-dicyclohexylurea was filtered off and, after removal of the solvent, crude product was recrystallized from methanol (**B1**), isopropanol (**M1**), or the mixture ethanol ethyl acetate (v/v = 1/1) (**M2**). Yields 67% of **B1**, 58% of **M1** and 72% of **M2** were obtained.

B1: ^{1}H NMR ($CDCl_3$), δ (ppm), 7.6 (4H, d, arom.), 7.15 (4H, d, arom.), 5.85 (2H, m, CH), 5.05 (4H, m, $-CH_2$), 2.5 (8H, m, $(CH_2)_2$). IR (KBr), ν (cm^{-1}), 3083, 1601–1495 (arom.), 2999–2855 (CH_2), 1745 (C–O), 1643, 998, 915 (C–C_{aliph}), 1218, 1169, 1151 (C–O). Elemental analysis: calcd for $C_{22}H_{22}O_4$ C 75.40, H 6.34; found C 74.45, H 6.39%. **M1**: ^{1}H NMR ($CDCl_3$), δ (ppm), 8.15 (2H, m, arom.), 7.2 (6H, m, arom.), 5.85 (2H, m, CH), 5.05 (4H, m, $-CH_2$), 2.5 (8H, m, $(CH_2)_2$). IR (KBr), ν (cm^{-1}), 3109–3082, 1605–1508 (arom.), 3001–2856 (CH_2), 1746, 1732 (C–O), 1643, 998, 916 (C–C_{aliph}), 1287, 1189, 1166, 1081 (C–O). Elemental analysis: for $C_{23}H_{22}O_6$ C 70.03, H 5.63; found C 70.25, H 5.67%. **M2**: ^{1}H NMR ($CDCl_3$), δ (ppm), 8.2 (4H, m, arom.), 7.2 (8H, m, arom.), 5.85 (2H, m, CH), 5.1 (4H, m, $-CH_2$), 2.5 (8H, m, $(CH_2)_2$). IR (KBr), ν (cm^{-1}), 3109–3091, 1602–1498 (arom.), 3010–2846 (CH_2), 1752, 1739 (C–O), 1642, 915 (C–C_{aliph}), 1263, 1179, 1129, 1069 (C–O). Elemental analysis: calcd for $C_{30}H_{26}O_8$ C 70.02, H 5.10; found C 69.92, H 5.16%.

3.4. *Epoxidation*

Under continuous stirring, 5.42 g (0.022 mol, 70%) of *m*-chloroperoxybenzoic acid was added to a solution of 0.01 mol of diolefin (3.5 g of **B1**, 3.94 g of **M1** or 5.14 g of **M2**) in 80 cm^3 of dichloromethane. The mixture was heated at reflux for 48 h (the reaction was monitored by TLC). After cooling and subsequent filtration, the mixture was washed with 80 cm^3 of aqueous 5% Na_2SO_3, 80 cm^3 of aqueous 5% $NaHCO_3$ and 30 cm^3 of aqueous 30% NaCl. The dichloromethane layer was dried over $MgSO_4$ and evaporated. Recrystallization from methanol (**BU1**), isopropanol (**MU1**) or a mixture of ethanol and ethyl acetate (v/v = 1/1) (**MU2**) yielded the final products. Yields: 64% of **BU1**, epoxy number (EN) = 0.520 (calcd. 0.524); 63% of **MU1** EN = 0.463 (calcd. 0.469); 73% of **MU2** EN = 0.361 (calcd. 0.366).

BU1: ^{1}H NMR ($CDCl_3$), δ (ppm), 7.5 (4H, d, arom.), 7.1 (4H, d, arom.), 3.0 (2H, m, CH of epoxy), 2.7 (4H, m, CH_2 of epoxy), 2.55 (4H, m, CH_2), 1.9 (4H, m, CH_2). IR (KBr), ν (cm^{-1}), 3060, 1601–1492 (arom.), 2990–2928 (CH_2), 1752 (C–O), 1207, 1169, 1141 (C–O), 915, 839 (epoxide). **MU1**: ^{1}H NMR ($CDCl_3$), δ (ppm), 8.2 (2H, d, arom.), 7.2 (6H, m, arom.), 3.0 (2H, m, CH of epoxy), 2.75 (4H, m, CH_2 of epoxy), 2.55 (4H, m, CH_2), 1.9 (4H, m, CH_2). IR (KBr), ν (cm^{-1}), 3110–3071, 1603–1508 (arom.), 2996–2929 (CH_2), 1756, 1732 (C–O), 1276, 1183, 1163, 1143, 1075 (C–O), 916, 854-841 (epoxide). **MU2**: ^{1}H NMR ($CDCl_3$), δ (ppm), 8.2 (4H, m, arom.), 7.2 (8H, m, arom.), 3.0 (2H, m, CH of epoxy), 2.75 (4H, m, CH_2 of epoxy), 2.55 (4H, m, CH_2), 1.9 (4H, m, CH_2). IR (KBr), ν (cm^{-1}), 3109–3062, 1602–1498 (arom.), 2998–2927 (CH_2), 1753, 1737 (C–O), 1262, 1182, 1157, 1132, 1068 (C–O), 922, 855 (epoxide).

4. Results and discussion

Phase transitions were studied using both DSC and optical techniques. Representative DSC traces for **MU1** and **BU1** (for both heating and cooling cycles) are shown in figures 2 (*a*) and 2 (*b*), respectively. The DSC trace for **MU2** shows two curves, see figure 2 (*c*). The first curve (solid line) was recorded during continuous heating of the sample up to approximately 300°C. The compound shows a nematic phase in the temperature range 168–276.5°C. However, degradation of the material occurs gradually at temperatures above 200°C. The endothermic peak at approximately 120°C presumably corresponds to either conformational changes or to a molecular relaxation after the crystallization from solution. This peak does not appear in the DSC curve (dotted line) recorded during the second heating cycle, performed after stopping the first cycle at 200°C to prevent degradation. The temperatures of the phase transitions determined in the DSC measurements were confirmed by microscopy.

Optical microscopy observations (figure 3) enabled correlation of the DSC peaks with solid – liquid crystal phase transition to be made. The materials investigated were placed between glass plates with no orientation layers, as shown for **MU1** in figure 3 (*a*). The textures of **M1**, **MU1**, **M2** and **MU2** were characteristic of nematic phases, figure 3 (*a*). In the case of **BU1** two higher ordered phases were observed. The first displayed a texture with coexisting double-refracting lancets and pseudoisotropic regions, figure 3 (*b*). The texture of the second phase contains strongly double refracting lancets and regions with layers parallel to the slide, figure 3(*c*). Such textures could suggest the existence of smectic B and crystal E phases, respectively [9], but as the textures alone do not give sufficient information to determine the phase type unambiguously, our investigations were supplemented by WAXS measurements. In the case of the compound **B1** no mesophase was detected. The results of DSC and optical observations are summarized in table 1.

The WAXS measurements of samples in thin capillaries confirmed the conclusions drawn from

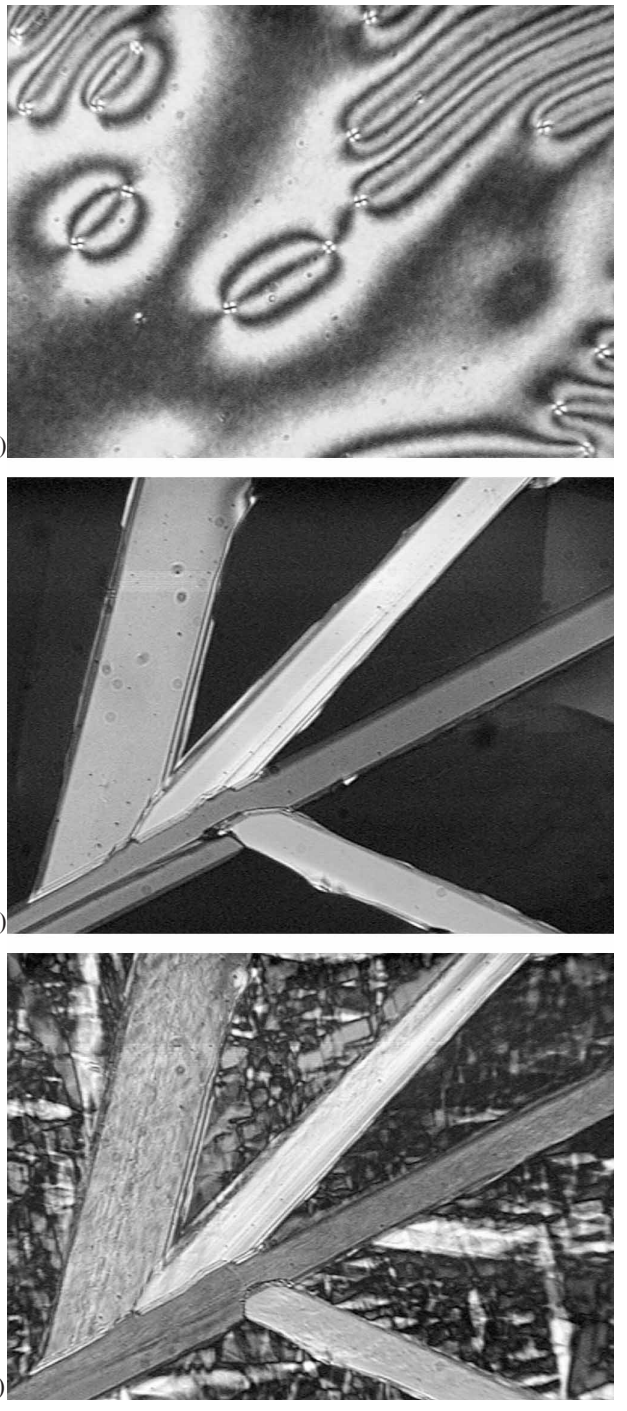

Figure 3. Optical textures of the compounds investigated, observed under a polarizing microscope between crossed polarizers; the samples were placed between glass plates: (*a*) a nematic texture of **MU1**; (*b*) a smectic B, texture of **BU1**; (*c*) a crystal E texture of **BU1**.

optical observations. For **M1**, **MU1**, **M2** and **MU2** similar patterns, and characteristic of the nematic phase [10], were obtained, figure 4 (*a*). The patterns obtained for **BU1** contain several sharp peaks, figures 4 (*b*) and 4 (*c*), implying a higher degree of ordering, in accord with the optical observations. The external magnetic field was applied in the equatorial direction in all cases.

Table 1. Phase transition temperatures for the compounds investigated, measured using DSC and optical microscopy. Cr = crystal/solid phase, N = nematic phase, I = isotropic liquid, SmB = smectic B phase, E = crystal E phase.

	Temperatures of phase transitions /°C	
Compound	Heating	Cooling
B1	Cr 126.8 I	I 126.2 Cr
BU1	Cr 103 SmB 114 I	I 113.2 SmB 102.8 E 99.5 Cr
M1	Cr 82.5 N 116 I	I 115 N 73.5 Cr
MU1	Cr 78 N 116 I	I 115 N 57 Cr
M2	Cr 164 N 275 I[a]	N 160.5 Cr[b]
MU2	Cr 168 N 276.5 I[a]	N 157 Cr[b]

[a]Material undergoes degradation
[b]After heating to 200°C

Considering the scattered intensity as a function of the scattering vector s ($s = 2\sin\theta/\lambda$, where θ is the scattering angle and λ is the wavelength [10]), it is possible to obtain the approximate values of several parameters of the measured system. The repeat distance l corresponding to s_m (the value of the scattering vector s at a diffraction maximum) may be computed as $l = 1/s_m$ [11]. This value, calculated for small angle peaks, may be directly interpreted as the approximate length of a molecule in nematics, and as the layer thickness in smectics. The position s_m of the wide angle reflections is related to the intermolecular distance d, but this relationship depends on the three-dimensional geometry of the system. For ordered nematics (as well as for smectic A and C phases) the geometry of random packing of parallel cylinders seems to be appropriate, which results in the formula $d = 1.12/s_m$ [11, 12]. In the case of smectic phases exhibiting a two-dimensional arrangement of molecules within layers, the calculation of molecular spacing will depend on the local cell structure (e.g. in the case of a hexagonal close packed arrangement the correct formula is $d = 1/(s_m \cos 30°)$ [13]).

The diffraction patterns for **M1** and **MU1**, figure 4 (*a*), are similar and show two pairs of diffuse reflections positioned at different scattering angles. The wide angle diffraction exhibits two crescent-shaped maxima in meridional positions, whereas the small angle reflections are equatorial. This is evidence of the orientation of the sample, induced by the external magnetic field. The lack of any other diffraction maxima indicates that there is no higher level ordering. This type of pattern is characteristic for ordered nematic phases [10]. Similar diffraction patterns were

also obtained by other authors (e.g. [12]) for different nematic materials. The director **n** of the structure is perpendicular to the imaginary line connecting the centres of both wide angle arcs [11, 12].

The patterns obtained for **M2** and **MU2** are essentially the same as for **M1** and **MU1**, indicating a nematic structure also in this case. In the case of **M2** four additional, weak diffraction maxima in the shape of diffuse dots are visible in the image; these maxima are located at the same angle with respect to the director **n**. This may indicate the formation of cybotactic groups, as proposed by de Vries [12]. The low intensity of the four reflections, which tend to disappear on increasing the temperature, suggest that the degree of ordering due to the cybotactic groups is small and they have only a very limited, local extent. This kind of ordering was not detected in the case of **MU2**. However, both epoxy structures (**MU1** and **MU2**) display only very weak small angle maxima and thus the absence of additional reflections could not be determined with absolute certainty.

The patterns obtained for BU1 are significantly different. The images recorded at 106 and 102°C, figures 4 (*b*) and 4 (*c*), respectively, have different features and confirm the existence of two distinct phases in this compound, as suggested by the DSC and optical observations. These two diffraction patterns will be discussed separately.

The image shown in figure 4 (*b*) exhibits one sharp ring positioned at $s \sim 2.2\,\mathrm{nm}^{-1}$. The ring is divided into two arcs which is the result of molecular orientation due to the magnetic field. The sharpness of the ring is evidence of a two-dimensional lattice within the layers, in contrast to the liquid-like layers of smectic A and C phases, for which a diffuse ring would be observed. The presence of only one such ring has often been used as an indication of a smectic B phases [13–15]. This kind of structure assumes the hexagonal arrangement of the molecules within the smectic layers [13]. The calculation of the distance between molecular planes for $s = 2.2\,\mathrm{nm}^{-1}$ gives a value of $l \sim 0.45\,\mathrm{nm}$, which is equivalent (for a hexagonal lattice) to an intermolecular spacing of $d \sim 0.52\,\mathrm{nm}$. Following the arguments of de Vries [13], a comparison of this value with the dimensions of the molecule indicates that the molecules are too closely packed to be able to rotate freely along their long axes. Thus the molecular arrangement is most likely a 'herring-bone' structure and the rotations about the long axes are rather co-operative.

The small angle reflections are due to inter-layer scattering. They appear as sharp spots in the image. This kind of reflection indicates the existence of rigid, well oriented smectic layers, which is the result of the strict molecular arrangement inside the layers [13]. The visibility of strong first order and weak second order maxima may suggest that the layers are arranged in a very regular manner, but there is a small disorder within the layers along the direction of the molecular axes [16]. The calculation of the layer width from the scattering vector value of $s \sim 0.42\,\mathrm{nm}^{-1}$ gives the value of $l \sim 2.38\,\mathrm{nm}$. This value is very close to the theoretical length of the **BU1** molecule (table 2) so we may expect that the molecular axes are perpendicular to the layers.

The X-ray image obtained for the other mesophase of **BU1** (at a lower temperature) displays a few features similar to the preceding phase, figure 4 (*c*). The small angle reflections form a spotty ring due to the rigid layers and a few second order reflections. The position of the ring is the same as in the previous case, which again indicates the arrangement of the molecules normal to the layers. The wide angle reflections are also sharp, indicating the regular arrangement of molecules within the layers. However, a closer analysis of the wide angle reflections shows that this is indeed a different type of mesophase. Firstly, the single sharp ring visible in figure 4 (*b*) is now separated into two separate rings. The rings are very close to each other—their separation does not exceed $0.15\,\mathrm{nm}^{-1}$. For that reason the presence of the second ring may be overlooked in the integrated plot $I(s)$, figure 5 (*b*), but the reflections belonging to both rings are clearly seen in the two-dimensional image, figure 4 (*c*). Secondly, another diffraction ring is now present at $s \sim 2.86\,\mathrm{nm}^{-1}$. The intensity of this ring is rather low, but it is clearly visible in the integrated plot $I(s)$, figure 5 (*b*). Assuming the orthorhombic local cell of the structure, these three rings may be indexed as 1 1 0, 2 0 0 and 2 1 0 reflections (starting from lower to higher angles). There is a difference with the smectic B case, in which a truly hexagonal local cell results in superimposing the 1 1 0 and 2 0 0 reflections [14].

A comparison of the diffraction pattern with the results presented in [14] may suggest the formation of a crystal E phase. This phase is characterized by a higher correlation between molecules than in the SmB phase, consistent with its occurrence at lower temperatures [15]. Another characteristic feature of this phase is the arrangement of the molecules in a stretched hexagonal lattice [13]. In our case, the distance between the 1 1 0 and 2 0 0 reflections is very small, so the deviation from a true hexagon must also be small. This fact, as well as a general similarity of both X-ray patterns, means that both phases of **BU1** have similar internal structures. This is consistent with the conclusion drawn by de Vries [13] that the SmB and E phases (with molecules perpendicular to the smectic layers) are closely related. Very similar results were presented by Doucet [14] for other materials exhibiting the E–SmB transition.

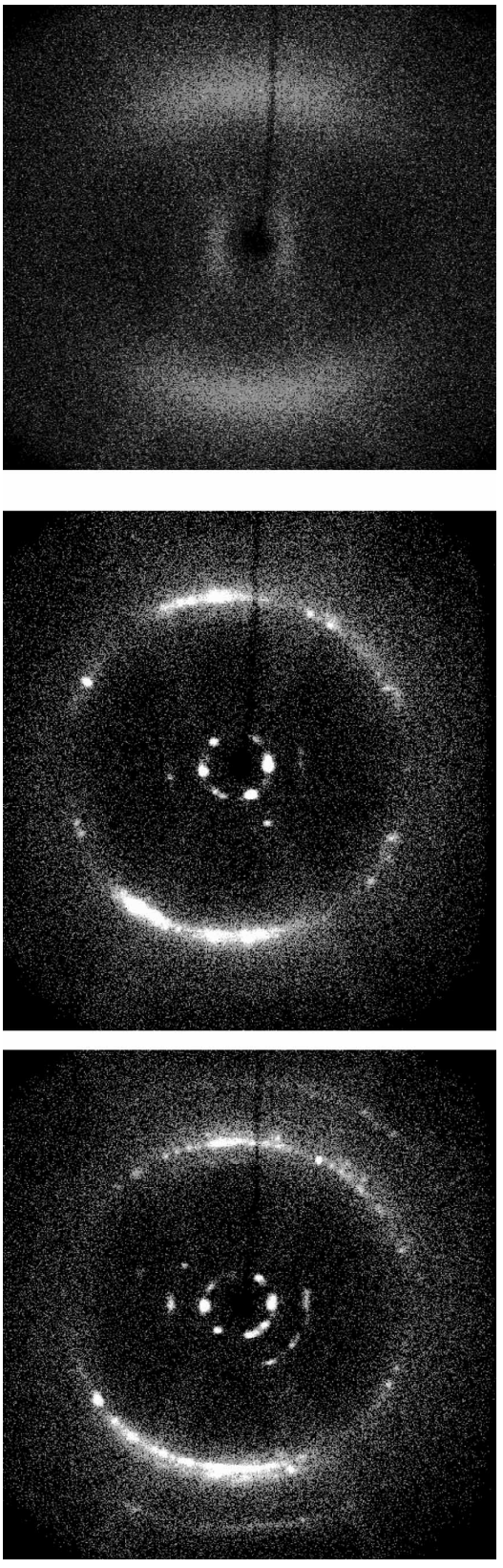

(*a*)

(*b*)

(*c*)

According to Doucet, the SmB phase is characterized by a rotational disorder of the molecules, so that locally there is a herring-bone packing of the molecules with three orientations of local domains. In contrast, in the E phase the herring-bone packing extends over long distances. This explanation seems reasonable also in our case.

The existence of long range order within the layers, as well as the correlation between adjacent layers (which may be concluded from the shape of the small angle reflections), suggest that this phase exhibits three-dimensional order and may resemble a graphite-like crystal phase. This is in agreement with the present state of knowledge, according to which all highly ordered smectic phases are actually genuine crystals [17]. Finally, it is noteworthy that this type of smectic polymorphism (E–SmB) has also been detected in other materials containing a biphenyl core [14, 18–20].

The theoretical structural studies of **BU1**, described in § 2, resulted in establishing the geometry of two different conformers (**BU1**$_{\alpha}$ and **BU1**$_{\beta}$). However, both conformers have very similar energy [4], so they probably exist concurrently in real materials. Other authors [21] have presented similar conclusions, based on NMR studies, for other liquid crystalline materials. Therefore, no obvious relationship between the two conformers and the formation of the two phases is apparent. However, more systematic structural studies of other compounds presenting the E–SmB transition are needed to investigate this further.

The experimental results from WAXS measurements (the values of the scattering vector s_m corresponding to the diffraction peaks and the calculated structural parameters) are presented in table 2 and compared with the lengths of the molecules obtained by *ab initio* methods, for the most extended conformers of the molecules [4, 5].

The results obtained from WAXS measurements are close to those obtained from quantum mechanical calculations. The observed differences are less than 10% of the calculated values. The simplest possible explanation of this fact may be that the long axes of the molecules are not aligned exactly with the global

Figure 4. Examples of WAXS 2D patterns. (*a*) **M1**, $T = 110^{\circ}$C; the diffraction pattern (two diffuse rings) is characteristic of an oriented nematic phase. (*b*) **BU1**, $T = 106^{\circ}$C; the diffraction pattern (one sharp wide angle ring, sharp and spotted small angle rings) is characteristic of an oriented smectic B phase. (*c*) **BU1**, $T = 102^{\circ}$C; the diffraction pattern (three sharp wide angle rings, one sharp spotted small angle ring and its second order) is characteristic of an oriented crystal E phase. The magnetic field was applied in the equatorial direction.

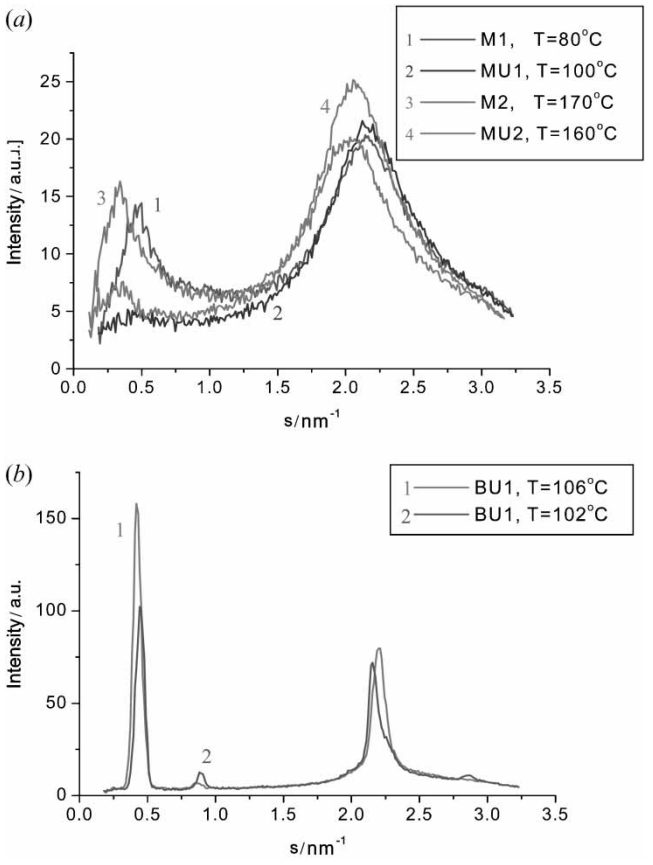

Figure 5. Plots of X-ray scattering intensity vs. scattering vector s. (*a*) Two diffraction maxima, typical for nematic materials, are visible for all the four compounds **M1**, **MU1**, **M2** and **MU2**. (*b*) The two plots correspond to the two phases observed for **BU1**. At small values of s one sharp peak and its second order are visible in both cases; at large values of s there is a single sharp peak at $T=106°C$ (SmB phase), but at $T=102°C$ this peak splits into two overlapping maxima ($s_1 \sim 2.15\,nm^{-1}$ and $s_2 \sim 2.25\,nm^{-1}$) and another small peak appears at $s_3 \sim 2.85\,nm^{-1}$—these three maxima indicate a crystal E phase.

director **n**. Instead, they are tilted by some angle β from the direction of **n**. We can then identify the correlation length s_m^{-1} obtained from WAXS measurements with the mean projection l_n of the molecular length l along the director. For the average value of $\beta \sim 30°$, which is quite reasonable for nematics, this model gives the values of $l_n \sim 0.9\ l$ [11], which is very close to our results. There are other factors which may influence the results. The diffraction peaks are not very sharp, which makes it difficult to determine the maximum accurately. In addition, the theoretical analysis suggested the possible co-existence of several conformers [4, 5], which would result in a smaller average length of the molecule. Furthermore, the *ab initio* calculations were carried out *in vacuo*, with no consideration of any intermolecular interactions. Taking all of this into account we may conclude that the results obtained are in satisfactory agreement with theoretical data.

Another quantity obtained from WAXS results (table 2) is the nearest neighbour distance, which is a little above 0.5 nm for all the molecules considered. Similar values have been found for a wide variety of compounds [11].

5. Conclusions

A two-stage method of synthesis for diepoxy compounds has been developed. With this method, six compounds (three divinyl and three diepoxy) were obtained. A mesophase was observed in five cases. The temperatures of the phase transitions were determined using DSC and polarizing microscopy. The mesophase types were identified by means of WAXS.

The compounds **M1** and **MU1** show a nematic phase in the temperature range 57–116°C. The compounds **M2** and **MU2** show a nematic phase at temperatures above 168°C. For these compounds degradation occurs before the nematic-isotropic phase transition can occur. **BU1** exhibits two phases during cooling: a smectic B

Table 2. Molecular lengths (l) and average intermolecular distances (d) calculated from the positions of WAXS maxima (s_m). Values of l are computed as $l=1/s_m$, values of d are computed as $d=1.12\,s_m^{-1}$ for **M1**, **MU1**, **M2** and **MU2** (random packing of cylinders), and as $d=s_m^{-1}/\cos 30°$ for **BU1** (hexagonal packing). The molecular lengths obtained from *ab initio* calculations (l_c) are presented for comparison. Symbols **α** and **β** denote two established conformers of **BU1**.

	WAXS – wide angle		WAXS – small angle		*Ab initio*	
Compound	s_m/nm^{-1}	d/nm	s_m/nm^{-1}	l/nm	l_c/nm	l/l_c
M1	2.15	0.52	0.45	2.22	2.48	0.90
MU1	2.18	0.51	0.42	2.38	2.36	1.01
M2	2.02	0.55	0.32	3.13	3.11	1.01
MU2	2.06	0.54	0.35	2.86	3.16	0.91
BU1	2.20	0.52	0.42	2.38	**α**: 2.33	1.02
					β: 2.31	1.03

phase in the temperature range 113.2–102.8°C and a crystal E phase in a narrow temperature range 102.8°C–99.5°C.

The experimental molecular lengths obtained from WAXS measurements are close to those obtained from quantum mechanical calculations (RHF method with 6-31G(d) basis set).

The authors are grateful to Prof. Witold Bartczak from the Institute of Applied Radiation Chemistry, Technical University of Lodz, for helpful discussions and technical support. Part of this work was supported by the Polish Committee for Scientific Research (KBN), grant no. 7 T09B 076 20. M. W. and B. M.-L. are grateful for fellowships from the Marie Curie Training Site at the Max Planck Institute for Polymer Research in Mainz.

References

[1] NAEMURA, S., 2001, *Displays*, **22,** 1.
[2] MOSSETY-LESZCZAK, B., WOJCIECHOWSKI, P., GALINA, H., and ULANSKI, J., 2001, *Polimery*, **5,** 374.
[3] FRISCH, M. J. *et al*., 1998, *Gaussian 98* (Pittsburgh, PA: Gaussian, Inc.).
[4] WLODARSKA, M., BAK, G., and BARTCZAK, W., 2002, *J. mol. Struct. (Theochem)*, **619,** 59.
[5] WLODARSKA, M., BAK, G. W., and BARTCZAK, W., 2002, *Theoretical ab initio studies on the conformations and dipole moments of selected divinyl and diepoxy monomers* (in Polish). Presented at the Polish Conference on Molecular Crystals, 17–21 September, 2002, Konstancin-Jeziorna, Poland.
[6] SCHLEGEL, H. B., 1982, *J. comput. Chem.*, **3,** 214.
[7] KANGAS, S. L., MENZIES, R. H., WANG, D., and JONES, F. N., 1989, *Polym. Prep.*, **30,** 462.
[8] BOCHWIC, B., 1975, *Preparative Methods in organic Chemistry* (in Polish), (Warsaw: PWN).
[9] DEMUS, D., and RICHTER, L., 1978, *Textures of Liquid Crystals* (Leipzig: VEB Deutscher Verlag fur Grundstoffindustrie).
[10] VICKERS, M. E., 1995, in *Scattering Methods in Polymer Science*, edited by R. W. Richards (London: Ellis Horwood), pp. 103–152.
[11] LEADBETTER, A. J., 1979, in *The Molecular Physics of Liquid Crystals*, edited by G. R. Luckhurst and G. W. Gray (London: Academic Press), pp. 285–316.
[12] DE VRIES, A., 1970, *Mol. Cryst. liq. Cryst.*, **10,** 219.
[13] DE VRIES, A., 1979, in *Liquid Crystals*, edited by F. D. Saeva (New York and Basel), pp. 1–73.
[14] DOUCET, J., 1979, in *The Molecular Physics of Liquid Crystals*, edited by G. R. Luckhurst and G. W. Gray (London: Academic Press), pp. 317–341.
[15] PETRIE, S. E. B., 1979, in *Liquid Crystals*, edited by F. D. Saeva (New York and Basel), pp. 163–203.
[16] DONALD, A. M., and WINDLE, A. H., 1992, *Liquid Crystalline Polymers* (Cambridge: Cambridge University Press).
[17] DE GENNES, P. G., and PROST, J., 1993, *The Physics of Liquid Crystals*, 2nd Edn (Oxford: Clarendon Press).
[18] COATES, D., GRAY, G. W., and HARRISON, K. J., 1973, *Mol. Cryst. liq. Cryst.*, **22,** 99.
[19] COATES, D., and GRAY, G. W., 1975, *J. Phys. (Paris), Colloq.*, **36:Cl,** 365.
[20] DEMUS, D., RICHTER, L., RUERUP, C. E., SACKMANN, H., and SCHUBERT, H., 1975, *J. Phys. (Paris), Colloq.*, **36:Cl,** 349.
[21] CHARVOLIN, J., and DELOCHE, B., 1979, in *The Molecular Physics of Liquid Crystals*, edited by G. R. Luckhurst and G. W. Gray (London: Academic Press), pp. 343–366.